Statistical and dynamical downscaling assessments of precipitation extremes in the Mediterranean area

Elke Hertig, Andreas Paxian, Gernot Vogt, Stefanie Seubert, Heiko Paeth, Jucundus Jacobeit

Angaben zur Veröffentlichung / Publication details:

Hertig, Elke, Andreas Paxian, Gernot Vogt, Stefanie Seubert, Heiko Paeth, and Jucundus Jacobeit. 2012. "Statistical and dynamical downscaling assessments of precipitation extremes in the Mediterranean area." *Meteorologische Zeitschrift* 21 (1): 61–77. https://doi.org/10.1127/0941-2948/2012/0271.

Meteorologische Zeitschrift, Vol. 21, No. 1, 061-077 (February 2012)

Article

Statistical and dynamical downscaling assessments of precipitation extremes in the Mediterranean area

ELKE HERTIG[1]*, ANDREAS PAXIAN[2], GERNOT VOGT[2], STEFANIE SEUBERT[1], HEIKO PAETH[2] and JUCUNDUS JACOBEIT[1]

[1]Institute of Geography, University of Augsburg, Germany
[2]Institute of Geography and Geology, University of Würzburg, Germany

(Manuscript received December 24, 2010; in revised form February 2, 2011; accepted February 28, 2011)

Abstract

Extreme precipitation events in the Mediterranean area have been defined by different percentile-based indices of extreme precipitation for autumn and winter: the number of events exceeding the 95th percentile of daily precipitation, percentage, total amount, and mean daily intensity of precipitation from these events. Results from statistical downscaling applying canonical correlation analysis as well as from dynamical downscaling using the regional climate model REMO are mapped for the 1961–1990 baseline period as well as for the magnitude of change for the future time slice 2021–2050 in relation to the former period. Direct output of the coupled global circulation model ECHAM5 is used as an additional source of information. A qualitative comparison of the two different downscaling techniques indicates that under the present climate both the dynamical and the statistical techniques have skill to reproduce extreme precipitation in the Mediterranean area. A good representation of the frequency of extreme precipitation events arises from the statistical downscaling approach, whereas the intensity of such events is adequately modelled by the dynamical downscaling. Concerning the change of extreme precipitation in the Mediterranean area until the mid-21st century, it is projected that the frequency of extreme precipitation events will decrease in most parts of the Mediterranean area in autumn and winter. The change of the mean intensity of such events shows a rather heterogeneous pattern with intensity increases in winter most likely at topographical elevations exposed to the West, where the uplift of humid air profits by the increase of atmospheric moisture under climate change conditions. For the precipitation total from events exceeding the 95th percentile of daily precipitation, widespread decreases are indicated in autumn, whereas in winter increases occur over the western part of the Iberian Peninsula and southern France, and reductions over southern Turkey, the eastern Mediterranean area, parts of Italy and some North African regions.

1 Introduction

The Mediterranean area is regarded as a "climate change hot-spot" (GIORGI, 2006) being highly affected by future climate change compared to other regions of the world. This is mostly due to the assessed increase of the inter-annual precipitation variability as well as to a projected decrease of precipitation and an increase of temperature mainly during the dry season. Besides these considerations based on mean changes and changes in the inter-annual variability, measures of changes in extremes might even be more important, since extreme events have a profound impact on society.

Observational changes in mean precipitation in different Mediterranean regions and their relationships with the large-scale atmospheric circulation have been studied quite extensively (e.g. DÜNKELOH and JACOBEIT, 2003, XOPLAKI et al., 2004 and MAHERAS et al., 1999 for the whole Mediterranean area; LOPEZ-BUSTINS et al., 2008 for the Iberian Peninsula; KUTIEL et al., 2001 for Turkey; BORN et al., 2008 for Northwest Africa). Also the number of studies focussing on extreme weather and climate events in the Mediterranean area has increased remarkably. In a study of extreme precipitation in the eastern half of the Mediterranean area KOSTOPOULOU and JONES (2005) find that the western part (Italian stations) shows positive trends towards increased extreme precipitation in the time period 1958 to 2000 while the eastern part of the study region (Balkan Peninsula, Cyprus and Turkey) is characterised by negative trends. Most notable is the steep positive trend characterising the Italian time series since the starting time of this increasing trend at the beginning of the 1970s (KOSTOPOULOU and JONES, 2005). Increases in heavy precipitation events were also presented by BRUNETTI et al. (2001) and ALPERT et al. (2002) for the central and western parts of the Mediterranean basin.

The question arises which future changes of precipitation have to be expected under increased greenhouse gas forcing. A major factor for generating precipitation in the Mediterranean area is the cyclonic activity. In this context RAIBLE et al. (2010) identify within the ECHAM5-model a decrease in the number of cyclones over the western Mediterranean area until the end of the 21st century under A2-scenario conditions. LIONELLO et al. (2008), using the regional climate model RegCM,

*Corresponding author: Elke Hertig, Institute of Geography, Universitaetsstrasse 1a, 86135 Augsburg, Germany, e-mail: elke.hertig@geo.uni-augsburg.de

DOI 10.1127/0941-2948/2012/0271

0941-2948/2012/0271 $ 7.45

find a decrease of cyclonic activity and extreme cyclones for the western as well as for the eastern Mediterranean area in winter. Associated with this decrease, a general rainfall reduction over the Mediterranean area is simulated. GIORGI and LIONELLO (2008) show by means of an ensemble of climate change simulations that essentially the whole Mediterranean area will be affected by pronounced decreases of mean precipitation in autumn. Also HERTIG and JACOBEIT (2008) assess by means of statistical downscaling techniques that at the beginning of the rainy season in October/November most of the Mediterranean area will be affected by mean precipitation decreases in the period 2071–2100 compared to the time period 1990–2019. But GAO et al. (2006) report positive precipitation changes in autumn south of the Alps, east of the Pyrenees and Jura Mountains, and over the eastern Hellenic Peninsula. In winter projected increases of precipitation are restricted to the Iberian Peninsula and parts of Italy under increased greenhouse warming conditions (HERTIG and JACOBEIT, 2008; GIORGI and LIONELLO, 2008). Gao et al. (2006) also assess DJF precipitation increases for most of France, the Alpine region and south-eastern Europe due to increased Atlantic storm activity. In contrast to that, the climate change projections point to substantial precipitation decreases during winter for the eastern and southern Mediterranean areas.

In a future climate influenced by increasing greenhouse gases, climate models continue to confirm the earlier results that precipitation intensity (i.e. more precipitation per precipitation event) is projected to increase over most regions of the world due to the nonlinearities involved within the Clausius-Clapeyron relationship (MEEHL et al, 2007). Particularly in the subtropics intense and heavy episodic rainfall events with high runoff amounts are assessed to be interspersed with longer relatively dry periods with increased evapotranspiration (MEEHL et al, 2007). As an overall picture of future climate change in terms of precipitation extremes, TEBALDI et al. (2006) identify, under the consideration of nine different Atmosphere-Ocean General Circulation Models, the northern Mediterranean regions as areas with increases whereas the southern and eastern Mediterranean regions will mostly be affected by decreases until the end of the 21st century. According to TEBALDI et al. (2006) the reasons for this pattern are likely related to proportionately more precipitation and higher precipitation intensity in areas of existing storm tracks and associated dynamical moisture convergence resulting from the greater moisture holding capacity of the warmer air, and also due to a slight poleward shift of the midlatitude storm tracks. Also KENDON et al. (2010) find in a study with the Hadley Centre HadAM3P model that the anthropogenic warming leads to significant increases in wet day intensity and extreme precipitation over much of Europe in winter. By contrast, wet day frequency is projected to decrease with warming over much of southern Europe, reinforced by soil moisture changes. Increases in extreme precipitation are supposed to extend further south in Europe than increases in mean precipitation, largely reflecting the changes in wet day frequency. However, for southern Spain Kendon et al. (2010) detect significant decreases in precipitation mean, intensity and extremes. FREI et al. (2006) assess a general tendency towards decreases of precipitation extremes for the whole Iberian Peninsula in winter. Results from the STARDEX project (Statistical and regional dynamical downscaling of extremes for European regions) indicate decreases in most indices of extremes in autumn for western Iberia and Greece. A remarkable exception is the east coast of Spain exhibiting October/November increases in all the different assessment versions. KENDON et al. (2010) judge that an increase in extreme precipitation over Europe as a whole is a reliable modelling result and dominated by increasing specific humidity along with further warming. The magnitude of this increase, however, remains uncertain. At the local scale, an enhanced increase or a decrease due to changing circulation patterns (e.g. a significant shift in the Atlantic storm track) is considered to be possible.

Apart from the fact that climate models are the only possibility to assess future climate conditions, it must be emphasized that major uncertainties are still inherent in global and regional climate models. Those are associated with the spatial and temporal resolution, the corresponding issue of discretisation and parametrisations (e.g. cumulus parametrization schemes analysed by EMORI et al., 2005), the reproduction of sea surface-temperatures, soil moisture (DIRMEYER et al., 2006), the account for stratospheric processes (DAI, 2006), the nesting technique of regional climate models and especially the problems of unknown initial conditions of corresponding variables (PAXIAN et al., in review). Particularly in the consideration of extreme events taking place at a local scale, interpretation of individual grid points must be subdued to a maximum of caution (DURMAN et al., 2001) keeping in mind the requirement of "skillful scales", as discussed by BENESTAD et al. (2008). A skillful scale is assumed to be reached at likely more than 8 grid points (VON STORCH et al., 1993).

For this reason in the present study several grid boxes are addressed as commonly known landscapes with the purpose of easier comprehension in the discussion. The main objective of this study is to provide a qualitative comparison between the different approaches without analysing the differences associated with individual grid points. In the present study the change of extreme precipitation events in the Mediterranean area until the mid-21st century is analysed using a regional dynamical model as well as a statistical downscaling approach. In this regard different percentile-based indices of extreme precipitation are considered to obtain a diverse small-scale picture of change. Section 2 describes the data used for this study, and section 3 gives the methodology. This is followed by the results in section 4 and a discussion and some conclusions in section 5.

2 Data

2.1 Observational data

2.1.1 Predictand

High-resolution precipitation data for the Mediterranean land areas were obtained from the E-OBS gridded dataset (HAYLOCK et al., 2008). This data set comprises daily values of precipitation on a 0.25° x 0.25° grid for European terrestrial areas. In a first step all grid boxes within the area from 27°N to 46.5°N and from the North Atlantic Ocean to 40.5°E have been considered which are characterised by a Mediterranean precipitation regime. The grid box selection follows that of DÜNKELOH and JACOBEIT (2003) in a study of Mediterranean precipitation variability in connection with large-scale circulation dynamics. Furthermore, considering the objective of calculating percentile-based indices for each grid box, data have been checked whether the time series contain less than 20 % missing values and less than 80 % zero-rainfall amounts. This mainly affects grid boxes in the area of northern Africa, which are excluded from further analysis. In this context it has to be emphasized that the utility of the gridded data is generally reduced over northern Africa due to the very poor station coverage over this area (HAYLOCK et al., 2008). Altogether the selection procedure results in 2857 grid boxes for autumn and in 2825 grid boxes for winter.

The observation-based data are used for the 1950–2006 period. Despite the fact that the wet season in the Mediterranean area generally extends from September to May, this paper only focuses on the two main rainy seasons autumn (September to November) and winter (December to February), being those seasons with the highest amounts of extreme precipitation in many parts of the Mediterranean area. The two seasons are handled separately in all subsequent analyses.

Different percentile-based indices of extreme precipitation are used for each grid box with a seasonal resolution: the number of events exceeding the 95th percentile of daily precipitation from the reference period 1961–1990 (R95N), percentage (R95T), total amount (R95AM) and mean daily intensity of precipitation (SDII95p) from these events (see MOBERG et al., 2006 and Table 1). Thus, different indices are available to characterize changes in the frequency and intensity of heavy rainfall events. In this context one has to keep in mind that the 95th percentile of daily precipitation is a rather moderate index to define the area of extremes within the whole precipitation distribution. However it is chosen in the present study because it includes a larger number of events, easing a sound statistical analysis. To account for the specific characteristics of the Mediterranean rainfall regime, particularly its spatial variability as well as its large intra- and inter-annual variability, only days with a minimum rainfall amount of 0.1mm are included in the calculations. For large parts of the Mediterranean area the mean total number of days with precipitation in the period 1961–1990 lies in the range of 40 to 50 days in the winter season, with the prominent exception of the eastern part of the Iberian Peninsula, the eastern Atlas Mountains and the Mediterranean coast of France, where the total number of days with precipitation adds up to only 15 to 20 days per winter season. In autumn a northwest-southeast gradient becomes evident with higher total numbers of about 30 to 40 precipitation days over the north-western parts of the Iberian Peninsula, Italy, and the Dinaric Alps, whereas the south-eastern Mediterranean area, for instance Israel and Egypt, has only 5 to 10 days with precipitation. From the total number of days with precipitation it can easily be inferred that the number of events exceeding the 95th percentile lies in the range of one day up to three days depending on the region and the season being considered.

To give further insight into the general characteristics of extreme precipitation in the Mediterranean area, Figure 1 shows the median of the daily 95th percentiles of precipitation in autumn and in winter for the reference period 1961–1990. From the upper part of Figure 1 it becomes apparent that in autumn high values of the 95th percentile of precipitation occur along the Mediterranean coast from north-eastern Spain, southern France, up to the region around the Gulf of Genoa. Also the western areas of the Dinaric Alps stand out as an area of high heavy rainfall amounts. In winter (lower part of Figure 1) high values of the 95th percentile can be seen over the north-eastern Mediterranean region, especially at the Mediterranean coast of Turkey. Overall the highest values in autumn and winter can be observed around the Gulf of Genoa and the north-western parts of the Iberian Peninsula with a median value of about 65 mm/day. The lowest values of the 95th percentile of precipitation can be found in regions off the preferred areas of cyclonic activity, like e.g. the continental parts of the Iberian Peninsula or the eastern side of the Apennine Mountains. Yet one has to keep in mind that the spatial interpolation, inherent to the gridded dataset, has a large impact on the magnitude of extremes. Thus the interpolation methodology has reduced the intensities of the extremes, with a reduction in all extremes higher than the annual 75th percentile for precipitation (HAYLOCK et al., 2008).

2.1.2 Predictors

Within the scope of statistical downscaling techniques, the choice of the predictor variables is of crucial importance. For example, HEWITSON (1998) and HERTIG and JACOBEIT (2008) have demonstrated how the downscaling results of future change in precipitation may alter significantly depending on whether or not humidity is included as a predictor. An important implication in this context is that while a predictor may or may not appear as important when developing the downscaling function under present climate conditions, the changes

Table 1: Percentile-based indices of extreme precipitation. The calculation is based on the reference period 1961–1990 considering days with precipitation amount >0.1 mm.

Index	Abbreviation
number of events exceeding the $> 95^{th}$ percentile of daily precipitation	R95N
percentage of total rainfall from events $> 95^{th}$ percentile	R95T
precipitation total from events $> 95^{th}$ percentile	R95AM
mean daily intensity from events $> 95^{th}$ percentile	SDII95p

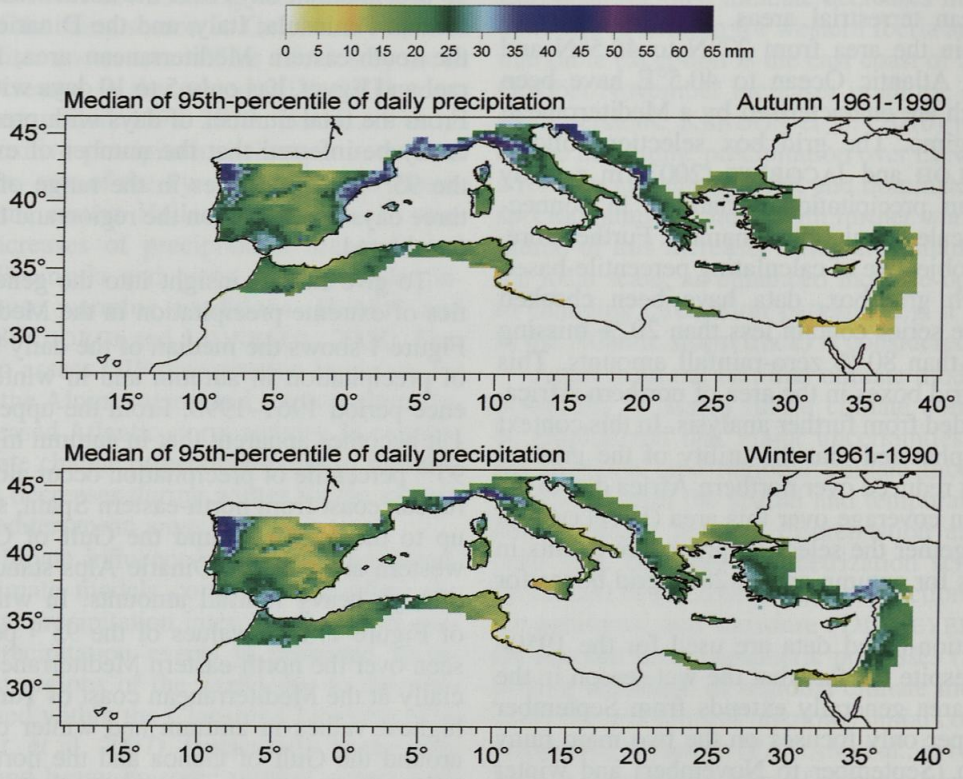

Figure 1: Median of the daily 95^{th} percentiles of precipitation in autumn (upper figure) and in winter (lower figure) for the reference period 1961–1990 from E-OBS data (0.25° spatial resolution).

in that predictor under a future climate may be decisive for determining the character and amount of climate change.

Geopotential height anomalies have to be regarded as primary factors for extreme precipitation conditions in the Mediterranean area (TORETI et al., 2010, CAVAZOS and HEWITSON, 2005). Furthermore, substantial improvements of statistical downscaling assessments for precipitation by the additional inclusion of humidity predictors are reported e.g. by CAVAZOS and HEWITSON (2005) for various locations including Spain, by HERTIG and JACOBEIT (2008) for the whole Mediterranean area and by BUSUIOC et al. (2008) for the Emilia-Romagna region.

In a study about the performance of reanalysis variables in statistical downscaling of daily precipitation by CAVAZOS and HEWITSON (2005), the meridional wind component appears in the list of the top variables in winter (in addition to geopotential heights and humidity variables), suggesting an influence from surface meridional synoptic systems on precipitation. Another key predictor for precipitation is relative vorticity, which is used in many downscaling studies (e.g. by KIDSON and THOMPSON, 1998; WILBY, 1998).

Large-scale atmospheric predictors for the statistical downscaling models were obtained from the NCEP/NCAR reanalysis project (KALNAY et al., 1996; KISTLER et al. 2001). The variables considered are geopotential heights of the 1000 hPa and 500 hPa levels for the area 20°N–70°N and 40°W–50°E, grids of 850 hPa and 700 hPa-specific as well as relative humidity, 850 hPa and 700 hPa-U-wind and V-wind components, and 1000 hPa-relative vorticity for the area 27.5°N–52.5°N and 12.5°W–42.5°E (horizontal resolution of 2.5° x 2.5° in each case). The limits of the larger area for the circulation-related predictors incorporate the major influences on the Mediterranean area, especially the mid-latitude westerlies in the upstream area. Tests with dif-

ferent sizes of the domain showed that for the other predictor variables (humidity, wind components, vorticity) a smaller size, concentrated over the target area itself, works better in terms of the subsequent dimensional reduction to meaningful principal components (PCs) and the further processing of the PCs in canonical correlation analysis (for details see section 3).

In conclusion it should be noted that the list of predictor variables is not exhaustive, further predictors might be selected, like for example GCM-simulated precipitation as a predictor for small-scale precipitation, like it was done for example by SCHMIDLI et al. (2006) for the European Alps. Also sea surface temperatures, aerosols, and cyclonic activity play a major role for precipitation in the Mediterranean area. But since these variables still suffer from major deficiencies in the dynamical models, the present study focuses only on the more 'classical' predictor variables.

2.2 Model Data

2.2.1 Regional Climate Model

Simulated precipitation is derived from the hydrostatic regional climate model REMO. The dynamical model, developed at the Max-Planck Institute for Meteorology (MPI), is designed for applications at the synoptic scale (JACOB et al., 2007). The physical parameterizations are derived from the global circulation model ECHAM4 (ROECKNER et al., 1996). In the version used here the model domain is centred over Africa and extends from 30°W to 60°E and from 15°S to 45°N with a horizontal resolution of 0.5° and 20 hybrid vertical levels up to 25km height (PAETH et al., 2009). In this study we analyse the Mediterranean sector from 20°W to 45°E and from 25°N to 44°N. Two grid point rows ($\sim$ 1°) have been removed from the northern rim to avoid lateral boundary effects. The REMO simulations are nested into simulations of the coupled global circulation model (CGCM) ECHAM5/MPI-OM (ROECKNER et al., 2003, 2006; for details see the following section 2.2.2) for the time period 1960–2050. During 1961–2000 observed GHG emissions and sulphate aerosol conditions are applied. For 2001–2050 the IPCC SRES (Special Report on Emission Scenarios, NAKICENOVIC and SWART, 2000) A1B scenario and corresponding land cover change scenarios following a stochastic land-cover change model (PAETH et al., 2009) are considered.

PAETH and HENSE (2005) state that a considerable part of the climatic processes (means and inter-annual variability of seasonal mean temperature and precipitation) in the Mediterranean area are well reproduced by the REMO-model when forcing it with input data from global reanalysis data sets, because the region is strongly influenced by the large-scale extra-tropical circulation of the North Atlantic region. This conclusion is confirmed by SANCHEZ-GOMEZ et al. (2009) who find that the regional models considered in their study (including REMO) can reproduce the long-term means and the inter-annual variability over Europe and the Mediterranean. However, at day-to-day time-scales the models clearly degrade the large-scale circulation due to the model formulation (physics and dynamics), the nesting technique and the internal variability inherent to the RCMs. Furthermore, PAETH and HENSE (2005) also note a basic deficiency of climate models in producing too much rainfall events of low intensity, while underestimating the observed maximum daily extremes.

Correspondingly to the observation-based precipitation data (section 2.1.1) the percentile-based indices of extreme precipitation (R95N, R95T, R95AM, SDII95p) are also used for each grid box of the REMO- model.

2.2.2 Global General Circulation Model

Model output of the ECHAM5/MPI-OM-CGCM (ROECKNER et al., 2003, 2006) is used in this study. The forcing uses observed greenhouse gas emissions for 1950–2000 and SRES A1B scenario emissions from 2001 to 2050. For the 20th-century simulation and the A1B scenario simulation one particular run of the ECHAM5 model is used as boundary conditions for the regional model REMO as well as for the representation of the model predictors within the scope of the statistical downscaling approach. This is done to ensure the direct comparability of the regional climate model output and the statistical downscaling results. One particular focus of this paper is on the influence and relevance of different downscaling approaches (statistical and dynamical) for assessing Mediterranean extreme precipitation changes in the 21st century. Discussing intra- and inter-CGCM differences is beyond the scope of this paper.

In the context of the statistical downscaling approach, general data pre-processing includes the fitting of the horizontal resolution of the model output data (T42, ~1.875°) to those of the observed predictor data (2.5° x 2.5°).

With regard to the predictand, the percentile-based indices of extreme precipitation (R95N, R95T, R95AM, SDII95p) are also calculated for each grid box of the ECHAM5-model. Grid boxes at which the percentiles can not be calculated are omitted. These are mainly grid boxes in the southern area of the domain. The illustrations of the direct ECHAM5 output in Figures 2 to 5 use the original horizontal resolution (T42).

3 Methodology

3.1 Statistical downscaling approach

Principal component analysis (PCA, e.g. PREISENDORFER, 1988; VON STORCH and ZWIERS, 1999) is separately applied to the different percentile-based indices of extreme precipitation in autumn and in winter and to the different seasonal mean predictor fields of the NCEP/NCAR-reanalysis in order to remove linear dependencies between variables and to reduce dimensions

of the data. In the present study, S-mode (RICHMAN, 1986), orthogonally (Varimax-criterion) rotated PCAs are carried out for the observational period from 1950 to 2006 for five different calibration periods (see section 3.2). The higher PC-loadings can be interpreted as defining regions of similar extreme precipitation variability or more generally (as for the case of the predictors) as spatial centres of variation. The determination of the number of PCs to be extracted follows the approach of PHILIPP et al. (2007) and is based on the criterion that each PC has to be uniquely representative for at least one input variable. Representativeness is assumed when the maximum loading of a variable on a particular PC is at least one standard deviation greater than the other loadings of this variable on the remaining PCs; additionally, this maximum loading has to be statistically significant at the 95 % level.

Concerning the percentile-based indices of extreme precipitation, the approx. 2800 grid boxes are reduced to 16 up to 25 PCs with explained variances (EVs) of 68 % up to 89 %. Generally the number of extracted PCs is lower and the amount of explained variance is higher for the winter season compared to autumn, indicating a somewhat higher spatial homogeneity of extreme precipitation in winter. Depending on the particular season, the geopotential height fields are reduced to 8 up to 11 PCs with overall EVs between 90 % and 96 %. The specific and relative humidity fields (note the smaller domain of these variables compared to the geopotential height fields) are reduced to 10 up to 13 PCs, the wind components to 8 up to 11 PCs, and the vorticity fields to 13 up to 17 PCs, all of them with EVs of about 90 %.

Subsequently, the time series (PC scores) of the extreme indices for autumn and winter 1950–2006 are linked to the large-scale atmospheric circulation represented by their corresponding PC time series. Canonical Correlation Analysis (CCA, e.g. BARNETT and PREISENDORFER, 1987) is used to establish particular predictor-predictand relationships. The number of significant canonical correlation patterns is determined by Rao's F-test (RAO, 1973) with a significance level of 0.1. As a first step separate CCAs are performed with each predictor variable to preselect significant predictors within a specific predictor dataset. The pre-selection is done by looking at the higher predictor canonical loadings of the significant canonical correlations. Depending on the extreme index, predictor variable, season, and calibration period considered, the number of predictor variables of a specific predictor dataset is reduced to about one third to two third of the original total number of PCs. Within the multiple-type predictor CCAs a detailed analysis of the results revealed that the CCA performance in calibration and verification (see next section 3.2) is better when using all canonical correlations instead of only the significant ones. Therefore all available canonical correlations are used to assess the response of extreme precipitation to changes of the large-scale predictors. For this purpose the GCM model data is projected onto the existing PCs of the observational period to obtain new predictor time series. Subsequently precipitation characteristics under control run conditions and under enhanced greenhouse gas forcing, respectively, are calculated for the PC time coefficients of the extreme precipitation indices using the CCA-relationships. Then a spatial back-transformation of the assessment results to the original 0.25° x 0.25° grid is done via multiplying the assessed PC time coefficients by the initial PC loadings. Statistical assessment results in the following sections are shown for the back-transformed, fully resolved grid fields.

Cross-validation is applied in all statistical analyses to test the suitability of the relationships developed between large-scale predictor and small-scale predictand variables. The requirement to verify the statistical relationships and to consider possible instationarities leads to a particular ensemble approach for the statistical downscaling models as described in detail in HERTIG and JACOBEIT (2008). Briefly described, the statistical ensemble approach arises from the use of several different calibration and verification periods, respectively. This procedure yields ensembles of statistical models comprising different circulation and climate relationships. Thus, being an important advantage of this ensemble method, non-stationarities in the circulation and extreme rainfall relationships are particularly taken into account restricted, however, by the fact that the 57-year training data set is not long enough to sample all independent episodes of low frequency variability.

3.2 Calibration and verification

In order to test whether the statistical models contain an appropriate set of predictor variables that includes low-frequency climate behaviour which does not change significantly through time, the whole study period 1950–2006 is divided into five calibration periods, each comprising 47 years in autumn and 46 years in winter (because December of the last year has no subsequent January and February values to calculate the winter value). Each of the five verification periods comprises 10 years which are not included in the corresponding calibration periods: 1956–1965, 1966–1975, 1976–1985, 1986–1995, 1996–2005. The partitioning of the study period into various segments allows the systematic selection of those models which exhibit stable connections between the large-scale circulation and Mediterranean extreme rainfall.

Model performance in the calibration periods and in the verification periods is assessed by means of the correlation coefficients between modelled and observation-based extremes indices. Additionally the RV-value (reduction of variance) is calculated in the verification periods, being similar to the root mean squared skill score. The RV 'reference' in the present study is the mean of the observations from the verification sample. RV = 100 % would mean a perfect model, RV = 0 % implies no improvement compared to the simple use of the sample climatology, and RV > 0 % indicates some improve-

ment by the model results. In the present study all statistical models with RV > 0 pass the verification procedure and are subsequently used for the assessment of precipitation extremes under control run conditions and simulated future climate change.

3.3 Comparison between statistical and dynamical downscaling assessments

Results are examined for the 1961–1990 baseline period as well as for the changes in the future time slice 2021–2050 in relation to the former reference period. Since the horizontal resolution differs between the statistical downscaling approach (0.25°) and the regional dynamical model (0.5°), the comparison is mostly based on a visual examination of the results. The CGCM output of ECHAM5 is taken as an additional explanatory source since both downscaling techniques use ECHAM5 as large-scale forcing. In this context the percentile-based indices of extreme precipitation calculated directly from ECHAM5 as well as the large-scale atmospheric predictor fields of ECHAM5 have been examined.

However, the different resolution of the mentioned datasets (~1.875°, 0.5°, 0.25°) influences the qualitative comparison between them. The RCM resolves more small-scale processes than the GCM and thus creates more energy to produce rainfall events of higher intensity. Local station records reach even higher precipitation intensities. In order to have a closer look at the scale effect and the comparability of precipitation extremes of datasets at different spatial scales, the daily data of E-OBS and REMO is linearly interpolated to 2° resolution in order to approximately fit the range of ECHAM5 (T42 resolution). Likewise a corresponding statistical downscaling model is generated on the daily E-OBS data with 2° resolution. Note that the resulting grid boxes do not match spatially between the different datasets due to data availability (e.g. only grid boxes over land areas in E-OBS). In case of the statistical downscaling technique, the same approach as described in sections 3.1 and 3.2 has been applied to the up-scaled observational data. The results of this analysis are exemplary discussed and shown for the mean daily intensity from those events which exceed the 95th percentile (SDII95p) in section 4.2.5 and in Figure 4, respectively.

Furthermore, the significance of the resulting changes for the future time period 2021–2050 in relation to the reference period 1961–1990 is evaluated by the "signal-to-noise-ratio" (S/N-ratio, see for example RAPP and SCHÖNWIESE, 1995). The S/N-ratio is obtained by setting the mean difference of the two 30-year periods in relation to natural variability, represented by the standard deviation of the inter-annual variations within the earlier period. Grid boxes with a signal to noise ratio being greater than 1 reach an amount of change greater than the recent natural variability. Additionally, the two time intervals are tested for significant differences (95 % level) using the non-parametric U-test (MANN and WHITNEY, 1947).

4 Results

Section 4.1 describes the findings of the predictor screening within the context of the statistical downscaling approach. Results of the statistical downscaling as well as of the dynamical downscaling with REMO are mapped for the 1961–1990 modelled baseline period (section 4.2) as well as according to the magnitude of change for the future time slice 2021–2050 in relation to the former reference period (section 4.3).

4.1 Predictor selection

Within the statistical downscaling approach the quality of different predictors and predictor combinations is evaluated in terms of their performance within the calibration and verification procedure (see section 3.2). Different predictor sets are tested to determine the best-performing models for the assessment of future extreme precipitation in the Mediterranean area. 1000 hPa and/or 500 hPa-geopotential heights are included as predictor variables for each analysis. However, one has to keep in mind that in the control run of ECHAM5 the geopotential heights are increased over most of the Mediterranean area (HERTIG et al., 2010; RAIBLE et al., 2010). The strongest deviations are found over its western part. Thus the model seems to overestimate the Azores high and therefore the west-east gradient over the Mediterranean area in winter. This means that the atmospheric circulation is too zonal compared with observational reanalysis data, a well-known bias of all IPCC models (HOUGHTON et al., 2001).

Other potential predictors like humidity fields and air flow strength are included in various combinations. From the analysis of the different potential predictors and predictor combinations it is revealed that the performance for extreme precipitation in autumn and winter in the Mediterranean area is enhanced when the predictor 850 hPa-specific humidity is included in the downscaling models. From the other predictor variables reflecting the wide range of atmospheric properties related to the generation of precipitation (wind speed, wind direction, and relative vorticity), only the additional inclusion of 1000 hPa relative vorticity leads to a further improvement of the downscaling models.

Thus, from the analysis of the different potential predictors and predictor combinations it is revealed that the best performance for extreme precipitation in autumn and winter in the Mediterranean area is achieved with the predictor combination 500 hPa geopotential heights, 850 hPa-specific humidity, and 1000 hPa relative vorticity. For this combination between 6 up to 13 predictor variables serve as independent variables, depending on the extreme index, the season, and the calibration period considered. Within the CCA-models the amount of explained variances of the predict and canonical variates for the original extreme precipitation adds up to about 60 % to 70 %. With respect to all grid boxes (2857/2825 grid boxes in autumn/winter) about 95 % in autumn

(ranging from 2702 grid boxes (R95T) up to 2778 grid boxes (SDII95p)) and about 80 % in winter (ranging from 2257 grid boxes (R95AM) up to 2333 grid boxes (R95N)) yield at least one robust downscaling model for a specific extreme precipitation index. The higher rate in autumn points to a better performance of the statistical models in the autumn season compared to winter.

Since mostly for two to three out of five verification periods robust downscaling models can be established for a specific grid box, it becomes evident that there is a varying performance in the different verification periods, indicating an intra- to inter-decadal variability of predictability. As an average over all grid boxes for which downscaling models can be established, the correlation coefficients between the modelled extreme precipitation indices and the observation-based indices amount to 0.61 up to 0.79 in the calibration periods and to 0.44 up to 0.56 in the verification periods.

4.2 Results for the 1961–1990 control run period

In this section results of the statistical and dynamical modelling for the 1961–1990 baseline period are presented to judge the performance of the two regionalization techniques in the present-day climate.

4.2.1 R95N (1961–1990)

The results of the modelling of the number of events exceeding the 95th percentile of daily precipitation (R95N) reveal that in REMO the number of events is generally about one day greater compared to the statistical downscaling. Thus in REMO three to four days exceed the 95th percentile in the northern Mediterranean area in autumn 1961–1990, especially over the northern Iberian Peninsula, southern France, and the Dinaric Alps, whereas only two to three days pass the 95th percentile in the statistical assessments for the abovementioned regions. In the other parts of the Mediterranean area R95N in autumn lies in the range of one up to three days in REMO and between one and two days in the statistical downscaling. In winter REMO simulates three to four days exceeding the 95th percentile over almost the whole Mediterranean area, only the eastern coast of the Iberian Peninsula and the southern parts of Mediterranean North Africa show lower values of about two days. The statistical assessment shows exceedances of about three days in winter over the north-western Iberian Peninsula, southern Italy, the Dinaric Alps, and the Levantine region. In contrast to that, the eastern Iberian Peninsula, the Mediterranean parts of Algeria, around the Gulf of Iskenderun, the Rhodope Mountains, and the Po valley are assessed to have about one day of extreme precipitation during the winter season.

Summing up the results for R95N, the statistical downscaling approach yields a very small scale spatial pattern, closely resembling that of the original E-OBS dataset. Also the number of events itself is matched very well by the statistical downscaling, whereas REMO tends to overestimate R95N by about one day when compared to the E-OBS data. But higher numbers of R95N, as seen in REMO, also become apparent in the direct output from ECHAM5. This points to the fact that the dynamical models produce a higher total number of rain days per season, since R95N is directly related to the latter.

4.2.2 SDII95p (1961–1990)

Looking at the modelling results in Figure 2 concerning the mean daily intensity from the events which exceed the 95th percentile (SDII95p) in the time period 1961–1990, reveals that ECHAM5 (upper row of Figure 2) generally produces the lowest values of SDII95p, with maxima of 25 mm to 35mm in some western and northern grid boxes of the Mediterranean area. It is a known feature of ECHAM5 to underestimate the upper tail of the precipitation distribution in the southern European/ Mediterranean area. Thus, SILLMANN and ROECKNER (2008) report that the model underestimates the 95th percentile of precipitation by approximately 50 mm corresponding to 30 % on average compared to observations. The underestimation of extreme precipitation can also be seen in other indices, such as the maximum 1-day precipitation and the simple daily intensity index (SILLMANN and ROECKNER, 2008). Besides, due to the low resolution of the GCM, only the approximate spatial structure is reproduced, omitting the great topographic influence on precipitation intensities inherent to the Mediterranean area.

In contrast to ECHAM5, REMO produces large values of SDII95p, especially at the western slopes of the Cantabrian Mountains, Apennine Mountains, Dinaric Alps, and Taurus with values reaching more than 100mm/day (Figure 2b). In a study of FREI et al. (2006) about the performance of RCMs in the Alpine region, it is shown that REMO is able to reproduce the general pattern of extreme precipitation, at least during dynamically active seasons with the highest frequency of heavy precipitation occurring in autumn and with a characteristic mesoscale pattern, reflecting topographic details and the proximity of the Mediterranean Sea.

Figure 2c shows the results from the statistical downscaling assessments. Centres of high extreme precipitation intensities are indicated around the Gulf of Genoa with largest values of about 70 mm/day, the northern coast of the Adriatic Sea, over the north-western Iberian Peninsula, and, in winter, also at the southern coast of Turkey and the Levantine region. In contrast to that, the continental areas of the Iberian Peninsula stand out as regions with very low values of SDII95p (about 10 mm/event), both in autumn and in winter. Altogether the statistical downscaling results resemble very closely the gridded observational values which are plotted in Figure 2d. The spatial pattern as well as the absolute height of the SDII95p- values follow closely the values from

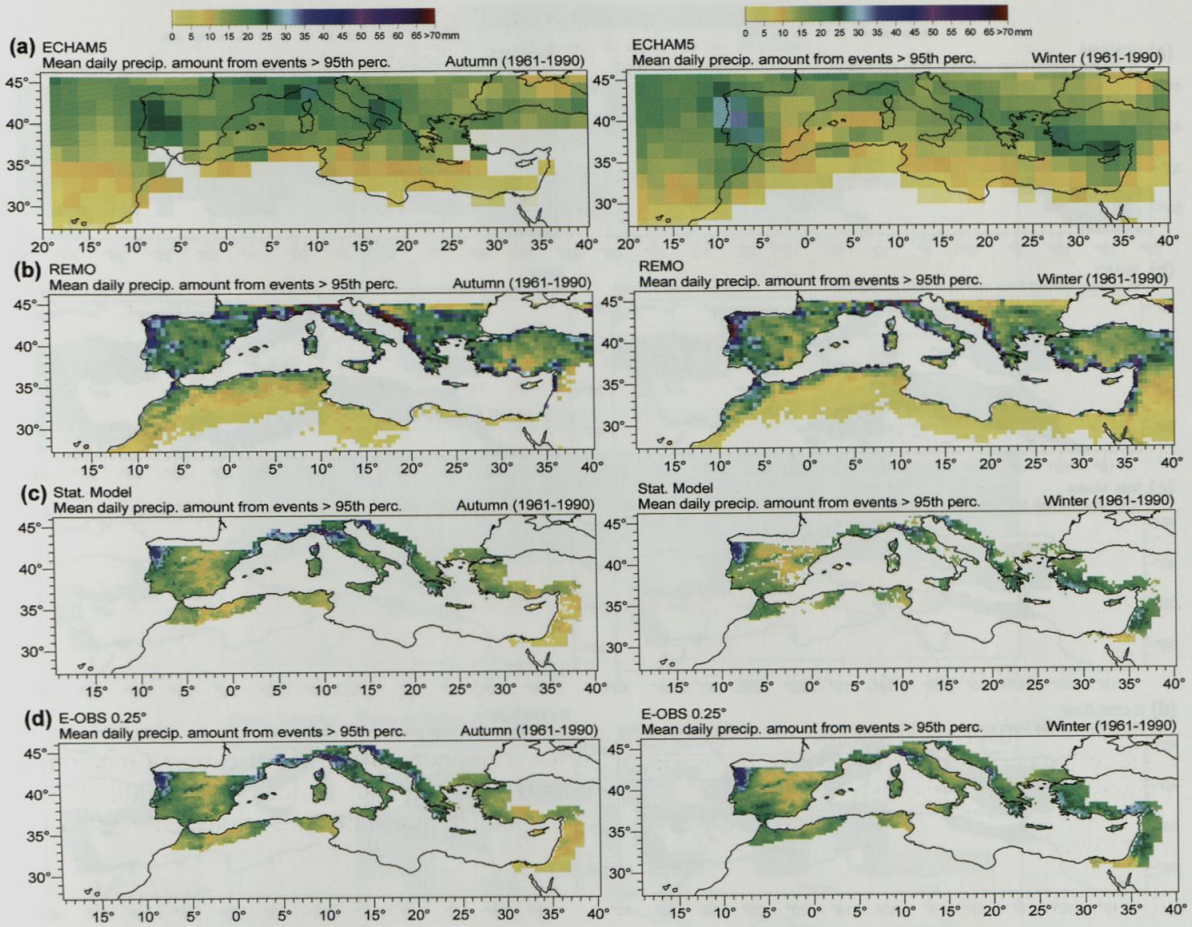

Figure 2: Mean daily precipitation intensity in mm/day from events >95th percentile of daily precipitation for autumn (left side) and winter (right side) 1961–1990 according to (a) ECHAM5, (b) REMO, (c) statistical downscaling, and (d) E-OBS 0.25°.

E-OBS, indicating that the statistical downscaling approach is highly capable to reproduce the observation-based values. But since the intensities of extremes are reduced within E-OBS due to the interpolation methodology, also the statistical downscaling results include this underestimation.

Comparing qualitatively the statistical downscaling results with the dynamical ones from REMO shows that both regionalization techniques yield a similar spatial structure of SDII95p in the Mediterranean area, with very good topographic details. But regarding the magnitude of extreme precipitation intensity, large differences occur, with generally higher values in REMO. The largest differences with values of up to 50 mm can be seen over the Dinaric Alps and some other mountain areas.

4.2.3 R95AM (1961–1990)

The precipitation total from events exceeding the 95th percentile of daily precipitation (R95AM) is the number of events exceeding the percentile (R95N) multiplied by the mean daily intensity from these events (SDII95p). The spatial structure of R95AM for the baseline period 1961–1990 (not shown) resembles closely the results of SDII95p (Figure 2). And, similar to SDII95p, the lowest values are obtained from ECHAM5 (maximum values of about 120 mm/season), whereas the highest values are modelled by REMO (up to 360 mm/season), with the statistical downscaling and E-OBS in between (maxima for both around 170 mm/season). But it is remarkable that R95AM from ECHAM5 is somewhat higher than expected from the sole examination of SDII95p. This is due to the comparatively high values of R95N in ECHAM5 (see section 4.2.1). In contrast to that, R95AM is reduced to some degree in the statistical assessments with higher SDII95p values being counteracted by lower R95N.Most striking are the results of REMO, producing very high values of R95AM, especially in mountainous areas, due to high numbers of R95N as well as high SDII95p-values.

4.2.4 R95T (1961–1990)

The most striking feature of the modelling results for the percentage of total rainfall from events >95th percentile (R95T) for the period 1961–1990 (Figure 3) is the fact that values of R95T are overall much higher in the two dynamical models ECHAM5 and REMO (with

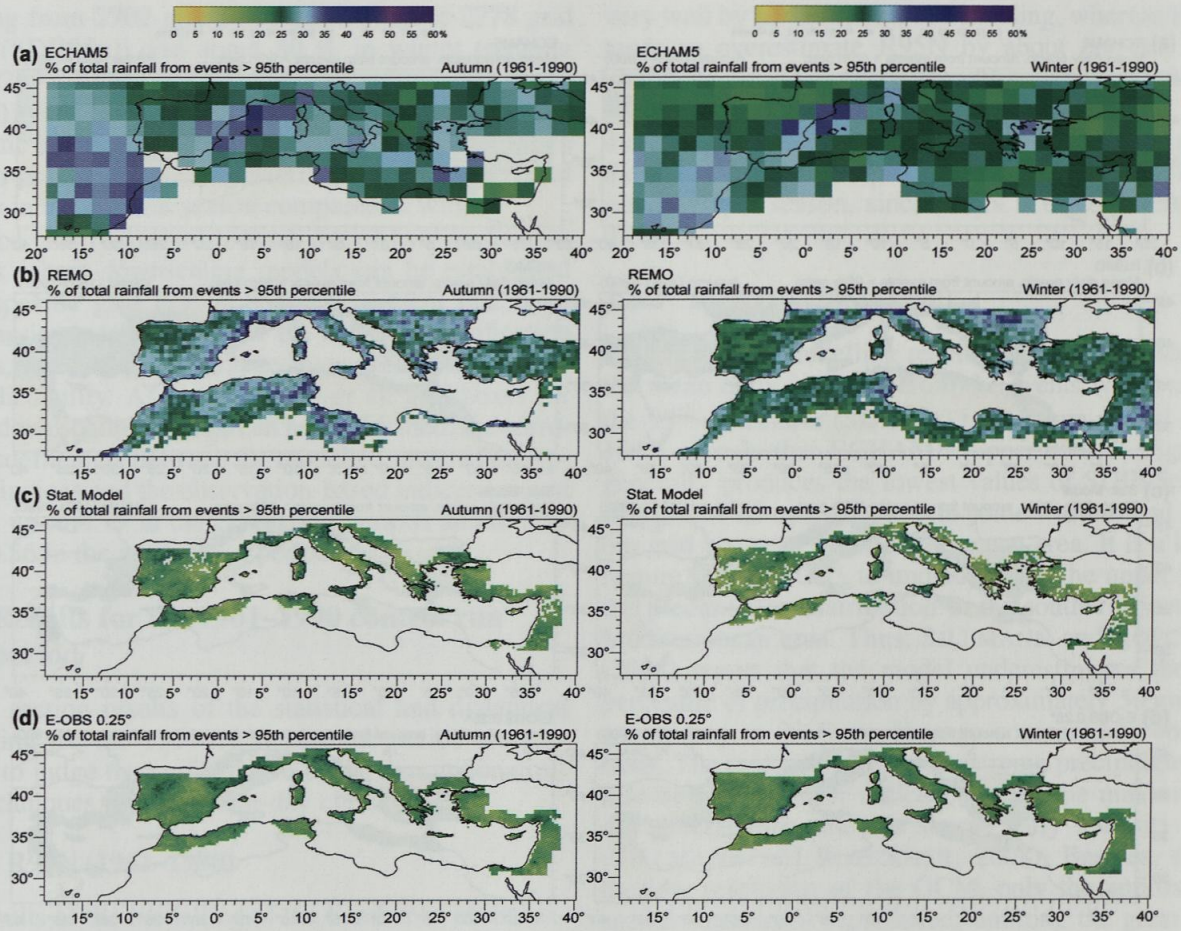

Figure 3: Percentage of total rainfall from events >95th percentile of daily precipitation for autumn (left side) and winter (right side) 1961–1990 according to (a) ECHAM5, (b) REMO, (c) statistical downscaling, and (d) E-OBS 0.25°.

values of about 25 % to 35 %) compared to the statistical assessments and the observation-based E-OBS dataset (with typical values of about 15 % to 25 %). But examining the results in detail reveals that there are different reasons for the similar results of the two dynamical models. In REMO the relatively high values of R95T are the consequence of a high wet day occurrence (see section 4.2.1) combined with great intensities of the extreme precipitation events (see section 4.2.2). In contrast to that, in ECHAM5 the high values of R95T do not result from great intensities of the extreme events but from high wet day occurrences and a low total precipitation amount, which is in some areas around two to three times lower than in the statistical model and REMO, respectively (not shown). Though the ECHAM5 projection produces about the same values of R95T like REMO, it takes much lower precipitation amounts as a basis for the calculation of R95T. Finally, the statistical downscaling results again closely follow the characteristics from E-OBS including a lower ratio of the precipitation total from events exceeding the 95th percentile to the total amount of precipitation when compared to REMO and ECHAM5, respectively.

4.2.5 Influence of the spatial resolution

The different resolutions of the models (ECHAM5: approx. 1.875°, REMO: 0.5°, statistical downscaling model: 0.25°) influence the comparison between them. The RCM resolves more small-scale processes than the GCM and this scale effect is partly responsible for the differences described in the above sections. SDII95p is taken as an example in order to have a closer look at the scale effect and the comparability of precipitation extremes at different spatial scales. For this purpose all highly-resolved daily precipitation data has been linearly interpolated to a 2° x 2° horizontal resolution prior to calculating the percentile- based index.

Figure 4 depicts (from top to bottom) the autumn SDII95p means of ECHAM5 on the original T42-resolution, REMO, the statistical downscaling model, as well as E-OBS on the up-scaled 2° horizontal resolution for the present-day time slice. The extreme precipitation intensities of the larger REMO 2° grid boxes are reduced in comparison to REMO with a 0.5° resolution, especially the maximum values, and resemble the ECHAM5 intensities. Nevertheless, REMO 2° yields higher intensities than ECHAM5 over Galicia, the Dinaric Alps and southern Turkey and lower intensities

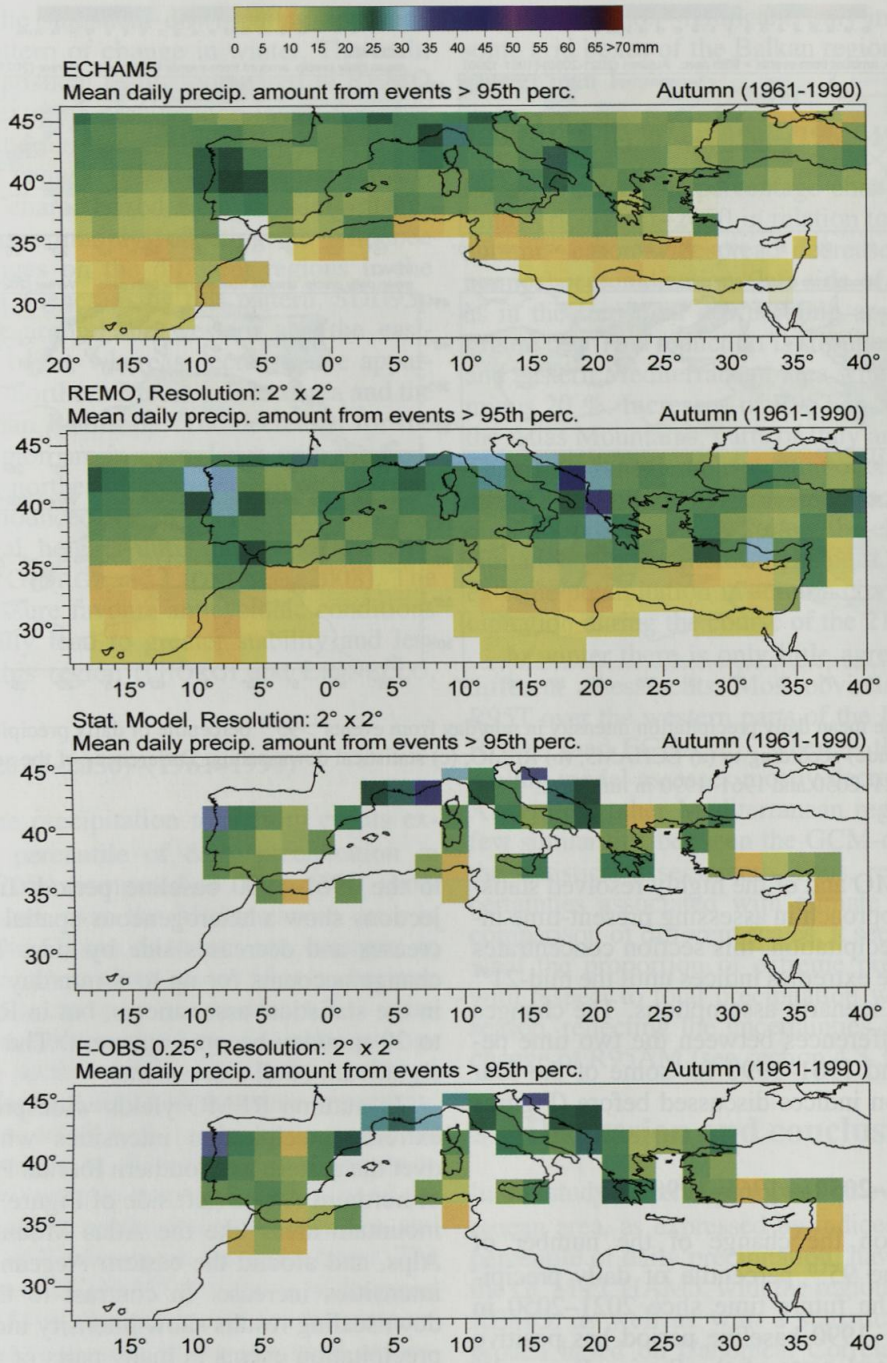

Figure 4: Mean daily precipitation intensity in mm/day from events >95th percentile of daily precipitation for autumn 1961–1990 according to (a) ECHAM5, T42-horizontal resolution, (b) REMO 2° resolution, (c) statistical downscaling 2° resolution, and (d) E-OBS 2° resolution.

over the Atlas Mountains. Thus, even after removal of the scale effect REMO shows more realistic extreme precipitation intensities than ECHAM5 which can be explained by a better representation of subgrid-scale processes. Therefore an "added value" of the regional climate model compared to the GCM- output can be stated. Generally both, scale effect and subgrid-scale processes of REMO 0.5°, mostly increase the SDII95p intensities compared to ECHAM5. Likewise the interpolation from 0.25° to 2° reduces the extreme precipitation intensities of E-OBS and consequently of the statistical downscaling model. Nevertheless, after removing the scale effect the extreme precipitation intensities of all different assessments are closer to each other compared to the results featuring different resolutions (see section 4.2.2).

4.3 Extreme precipitation changes until the mid-21st century

After examining the skill and drawbacks of the coarsely resolved GCM ECHAM5 as well as of the regional dy-

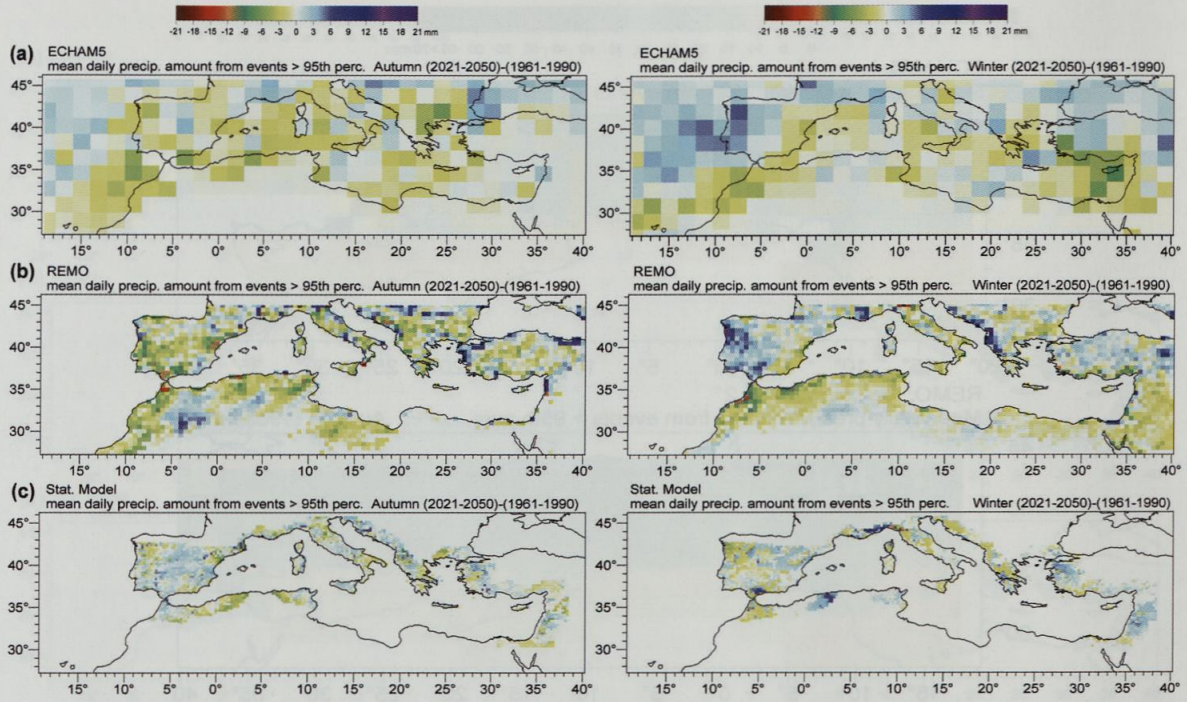

Figure 5: Changes of the mean daily precipitation intensity in mm/day from events >95th percentile of daily precipitation for autumn (left side) and winter (right side) according to (a) ECHAM5, (b) REMO, (c) statistical downscaling. Differences of the seasonal extreme index between the periods 2021–2050 and 1961–1990 in mm/day.

namical model REMO and of the highly resolved statistical downscaling approach in assessing present-time indices of extreme precipitation, this section concentrates on the changes of the extremes indices until the mid-21st century under A1B scenario assumptions. The changes are illustrated as differences between the two time periods 2021–2050 and 1961–1990 for some of the four extreme precipitation indices discussed before (Figures 5 and 6).

4.3.1 R95N (2021–2050)–(1961–1990)

In the winter season the change of the number of events exceeding the 95th percentile of daily precipitation (R95N) for the future time slice 2021–2050 in relation to the 1961–1990 baseline period has positive values over the central parts of the Iberian Peninsula, southern France and parts of the Dinaric Alps with a maximum increase of one day (not considering the non-Mediterranean region of the southern coast of the Black Sea with increases of up to two days (S/N-ratio > 1) according to dynamical model results of REMO). Beyond that all assessments (ECHAM5, REMO, and the statistical downscaling approach) indicate a slight decrease of R95N in the other parts of the Mediterranean area in winter and for almost the whole region in autumn.

4.3.2 SDII95p (2021–2050)–(1961–1990)

Figure 5 shows the change of the mean daily precipitation intensity from events exceeding the 95th percentile for the future time slice 2021–2050 in relation to the 1961–1990 baseline period. In general all projections show a heterogeneous spatial structure with increases and decreases side by side. The magnitude of change accounts for up to 8 mm/day in ECHAM5 and in the statistical assessments, but in REMO changes up to 20 mm/day become apparent. The changes are non-significant in all assessments.

In autumn REMO yields widespread reductions of extreme precipitation intensities which are strongest over the eastern and southern Iberian Peninsula and parts of northern Africa (left side of Figure 5b). Only in some mountain areas like the Atlas Mountains, the Dinaric Alps, and around the eastern Aegean Sea precipitation intensities increase. In contrast to that, the statistical downscaling results show intensity increases of extreme precipitation events in many parts of the Mediterranean area in autumn (left side of Figure 5c).

In the winter season REMO (right side of Figure 5b) projects an increase of SDII95p mainly in some western and northern Mediterranean regions, roughly in uplift areas of the topographical elevations. This result is also reported in a high-resolution climate change experiment over the Mediterranean area by GAO et al. (2006). Reductions of SDII95p in winter occur in REMO over the southern Mediterranean area being strongest over western North Africa. Considering the output of ECHAM5 (right side of Figure 5c) yields a similar tendency of SDII95p like in REMO. But it also becomes apparent that the resolution of ECHAM5 is too coarse to capture the fine-scale structure of the climate change signal as it becomes evident in the regional dynamical model.

The results of the statistical downscaling approach yield a different pattern of change in winter. The main difference of the statistical results compared to REMO is the reduction of extreme precipitation intensities over the north-western Iberian Peninsula as well as over the Dinaric Alps. The change of SDII95p in the statistical assessments is characterized by a mosaic with increases and decreases, mainly reflecting the influence of circulation changes on the different regions in the Mediterranean area. Generalising this pattern, SDII95p increases dominate around the western and the eastern Mediterranean basin, whereas decreases are apparent over the central-northern Mediterranean area and the north-western Iberian Peninsula. The decreases for the central-northern region are in accordance with the finding that the central-northern Mediterranean area depicts the centre of a pronounced rise in sea level pressure and 500hPa-geopotential heights until the end of the 21st century in winter (GIORGI and LIONELLO, 2008). The increased high pressure favours anticyclonic conditions and should generally lead to greater stability and less storm activity in this region (GIORGI and LIONELLO, 2008).

4.3.3 R95AM (2021–2050)–(1961–1990)

The changes of the precipitation total from events exceeding the 95th percentile of daily precipitation in the period 2021-2050 compared to 1961–1990 show widespread decreases over the Mediterranean area in autumn (not shown). These decreases are strongest in REMO with values up to about minus 50 mm, because a reduction of the occurrence (see section 4.3.1) coincides with a decrease of the intensity of extreme precipitation events (see section 4.3.2). Also in the statistical assessments decreases of R95AM dominate in autumn, but these are rather small with values up to minus 20 mm, because decreases of the extreme day frequency are counteracted by intensity increases. Only around the Gulf of Lyon, around the north-eastern Adriatic Sea, and the southern coast of Turkey weak increases occur. The direct GCM-output of ECHAM5 also shows widespread decreases of R95AM in autumn, except for the same areas of weak increases as seen in the statistical assessments.

In winter there is quite a good agreement between the different projections with increases of R95AM over the western part of the Iberian Peninsula and southern France, and with reductions of R95AM over southern Turkey, the eastern Mediterranean area, parts of Italy and some North African regions. But the agreement between the different assessment results only concerns the direction of change, which mainly reflects the pattern of change of R95N, whereas the magnitude of change can differ quite considerably, with the largest changes occurring in REMO again. Here the maximum increases reach values of about 120mm, whereas in ECHAM5 and in the statistical assessments the maximum increases amount to 50mm and 30mm, respectively. The changes are generally non-significant, only in the REMO results some grid boxes of the Balkan region show a S/N- ratio greater than 1.

4.3.4 R95T (2021–2050)–(1961–1990)

Figure 6 shows the percentage change of R95T for the time period 2021–2050 in relation to 1961–1990. In the autumn season widespread decreases occur in the dynamical regionalization (left side of Figure 6b) as well as in the statistical downscaling approach (left side of Figure 6c). This reduction is strongest over the southern and eastern Mediterranean area with values up to about minus 20 %. Increases of R95T in autumn appear over the Atlas Mountains, parts of Italy and southern Turkey. The partly considerable amount of change of R95T indicates that the change of extreme precipitation in autumn does not proportionally follow the change of mean precipitation. Rather there might be a stronger decline of extreme precipitation in autumn compared to mean precipitation during the course of the 21st century.

In winter there is only little agreement between the different assessments. Most obvious is the increase of R95T over the western parts of the Iberian Peninsula in REMO (and ECHAM5), whereas the statistical downscaling model assesses mostly decreases over this area. Also in the other Mediterranean regions there are only few similarities between the GCM-output, REMO, and the statistical assessments. Thus, regardless of the uncertainties associated with climate modelling and the comparison of different scales, it seems rather uncertain what the proportion of extreme precipitation amounts with respect to total precipitation will be in the winter season, reflecting the uncertainties in the magnitude of change of R95AM (see section 4.3.3).

5 Discussion and conclusions

In this study extreme precipitation events in the Mediterranean area, as expressed by indices based on the 95th percentile of daily precipitation, have been studied with the GCM ECHAM5, with the regional dynamical model REMO, as well as with a statistical downscaling approach based on Canonical Correlation Analysis. The analyses have been carried out for two Mediterranean wet seasons, autumn and winter, being those seasons with the highest amounts of extreme precipitation in many parts of this area.

Within the statistical downscaling approach the best models for the assessments of extreme precipitation indices in autumn and winter could be established by taking 500 hPa-geopotential heights, 850 hPa-specific humidity, and 1000 hPa-relative vorticity as large-scale predictors.

It could be shown that REMO seems to overestimate the number of events exceeding the 95th percentile (R95N), but produces a better representation of extreme precipitation intensities (SDII95p) compared to the statistical assessments. The first finding might be related

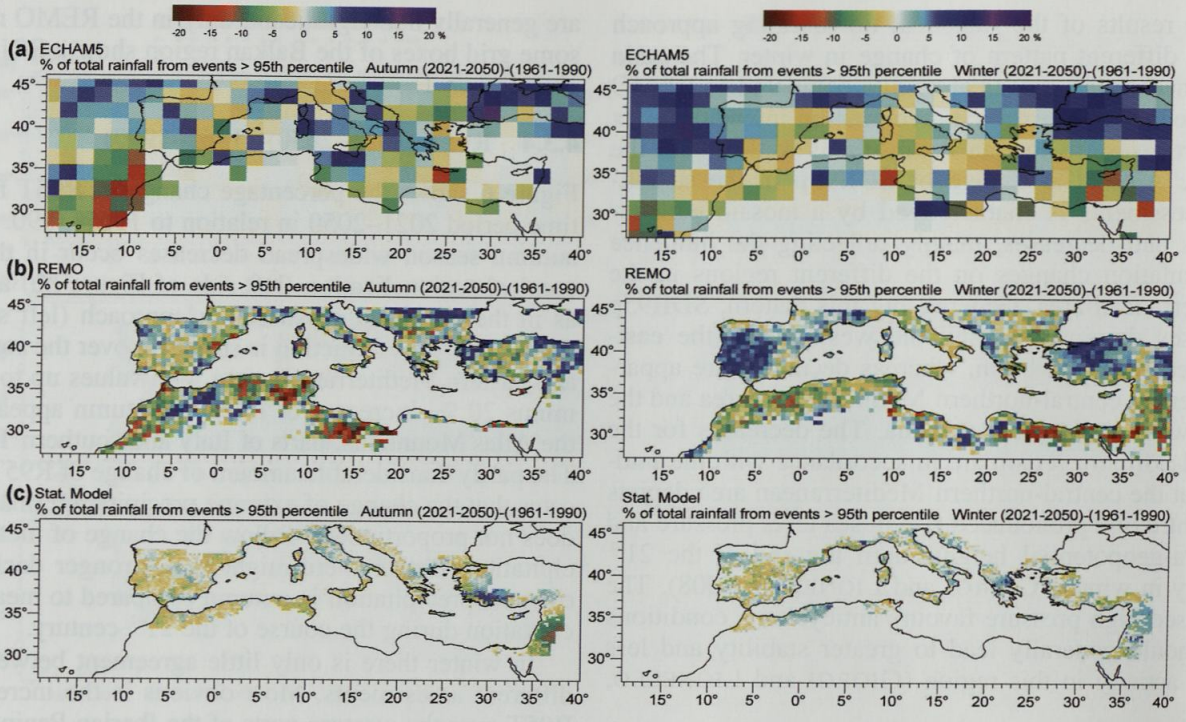

Figure 6: Changes of the percentage of total rainfall from events >95th percentile of daily precipitation for autumn (left side) and winter (right side) according to (a) ECHAM5, (b) REMO, (c) statistical downscaling. Differences of the seasonal extreme index between the periods 2021–2050 and 1961–1990 in %.

to the general problem of comparing precipitation results of different scales. Dynamical and statistical downscaling are performed on similar spatial scales (0.5° and 0.25°, respectively) but the latter is based on interpolated station records. PAETH and HENSE (2005) note that in the Mediterranean area the shape of the two-dimensional precipitation distributions is shifted towards higher values in REMO compared to grid-based observations. PAETH and DIEDERICH (2010) propose a statistical-dynamical weather generator containing orographic and stochastic correction terms to develop virtual station time series from regional climate model output and thus solve the problem of too frequent rainy days in the 50 km-grid boxes of REMO compared to local station observations. A follow-up study is planned to apply a weather generator to the REMO model output and to compare these results with the precipitation extremes of the previous study. The latter finding might be explained by a better representation of orographic effects in the non-linear dynamical downscaling model than in the statistical downscaling approach. Furthermore, HAYLOCK et al. (2008) point out that in the grid-based observations the extremes are reduced due to the interpolation methodology. Therefore it will be interesting to see whether station-based statistical assessments will provide a higher correspondence to the dynamical downscaling results regarding the magnitude of extreme precipitation intensities. This will also be part of future investigations.

Consequently, regarding the precipitation totals from events exceeding the 95th percentile (R95AM, the combination of R95N and SDII95p), the 'true' values might range between the higher dynamical results and the lower statistical assessments. This might also be valid for the percentage of total rainfall from events exceeding the 95th percentile (R95T).

With respect to the influence of the spatial resolution, the interpolation of REMO and E-OBS to ECHAM5 resolution removes the "scale effect". As a result the maxima of SDII95p are smoothed out and thus, the results of all different assessments are closer to each other than before based on different resolutions.

Overall, the least realistic description of extreme precipitation events in the Mediterranean area (as expressed by the 95th percentile of daily precipitation) is produced by the global ECHAM5 model, clearly pointing to the substantial benefits of downscaling exercises in the Mediterranean area. The comparison of the two different regionalization techniques indicates that for the present climate both the dynamical and the statistical techniques have skill to reproduce extreme precipitation in the Mediterranean area. But the question arises which is more correct under future climate conditions. Despite the fact that regional dynamical models clearly provide a better physical basis for climate change, different regional models still generate differences in downscaled changes (see e.g. FREI et al., 2006; DÉQUÉ et al., 2005). Statistical downscaling approaches are computationally inexpensive and yield in many cases simi-

lar skill compared to the dynamical approaches, but the assumption of stationarity in the predictors-predictand relationships under future climate change is not strictly verifiable, defining a particular vulnerability of statistical downscaling approaches.

Concerning the change of extreme precipitation in the Mediterranean area until the mid-21st century, it becomes apparent that for the number of events exceeding the 95th percentile the change in the period 2021–2050 is quite consistent between the different assessments (despite the different levels in the baseline period). Mainly slight decreases of the number of events exceeding the 95th percentile of up to about one day are indicated for the Mediterranean area in autumn and in winter.

The change of the mean daily precipitation intensity from events exceeding the 95th percentile shows a heterogeneous spatial structure with small-scale increases and decreases. Also the consistency between the different projections is only partly realised. While the pattern resulting from the dynamical model is largely affected by responses to the forcing of the complex topography of the region, the statistical downscaling results depend mainly on the changes of the large-scale circulation and humidity predictors. The synopsis of the different results indicates preferred increases of SDII95p in autumn at the eastern coasts of the Adriatic Sea and the Aegean Sea. In winter increases are most likely at topographical elevations exposed to the West, where the uplift of humid air profits by the increase of atmospheric moisture under climate change conditions. Reductions of SDII95p in winter can be seen mainly over the southern and eastern Mediterranean area.

The results from this study confirm findings presented in other papers, e.g. by KENDON et al. (2010) who show by means of the Had-AM3P model that over the Mediterranean area in winter the anthropogenic warming is likely to reduce the occurrence of precipitation events. According to the authors this is due to a reduction in relative humidity. By contrast, the implication that increases in specific humidity are expected to increase the intensity of individual precipitation events when they occur (MEEHL et al, 2007), can only partly be confirmed for the Mediterranean area. This might be due to the fact that the intensity of heavy precipitation events in the Mediterranean area is not only governed by the moisture availability, but also by further factors like the characteristics of the associated circulation patterns, the sea surface temperatures of the Mediterranean Sea, and topographic details of the landmasses.

For the precipitation total and for the percentage of total rainfall from events exceeding the 95th percentile of daily precipitation, widespread decreases in the period 2021–2050 compared to 1961–1990 are found in autumn. This reduction is strongest over the southern and eastern Mediterranean area. In winter the different projections indicate increases of R95AM over the western part of the Iberian Peninsula and southern France, and reductions of R95AM over southern Turkey, the eastern Mediterranean area, parts of Italy and some North African regions.

Overall the present study has highlighted a very complex pattern of extreme precipitation changes in the Mediterranean area. Keeping in mind the shortcomings of global and regional climate modelling and statistical downscaling in estimating precipitation extremes, the present-day assessments and future projections of this study face several uncertainties. Much additional work is necessary to reduce uncertainties, e.g. by applying station-based statistical assessments or a statistical-dynamical weather generator. Within the scope of the statistical downscaling, also synoptic approaches will be considered, including a representative description of the probability density function for daily precipitation as done by BENESTAD (2010) for Oslo, or following the approach of VRAC and NAVEAU (2007) who fitted the Gamma and Generalized Pareto distributions to daily precipitation data of Illinois. The efforts are especially important because the Mediterranean area is a highly vulnerable region in the scope of the anticipated global climate change.

Acknowledgments

Financial support is provided by the DFG (German Research Foundation). We acknowledge the E-OBS dataset from the EU-FP6 project ENSEMBLES (http://ensembles-eu.metoffice.com) and the data providers in the ECA&D project (http://eca.knmi.nl).

References

ALPERT, P., T. BEN-GAI, A. BAHARAD, Y. BENJAMINI, D. YEKUTIELI, M. COLACINO, L. DIODATO, C. RAMIS, V. HOMAR, R. ROMERO, S. MICHAELIDES, A. MANES, 2002: The paradoxical increase of Mediterranean extreme daily rainfall in spite of decrease in total values. – Geophys. Res. Lett. **29**, 311–314.

BARNETT, T., R. PREISENDORFER, 1987: Origins and levels of monthly and seasonal forecast skill for the United States surface air temperatures determined by canonical correlation analysis. – Mon. Wea. Rev. **115**, 1825–1850.

BENESTAD, R.E., 2010: Downscaling precipitation extremes. Correction of analog models through PDF predictions. – Theor. Appl. Climatol. **100**, 1–21.

BENESTAD, R.E., I. HANSSEN-BAUER, D. CHEN, 2008: Empirical-statistical downscaling. – World Scientific Publishing Co. Pte. Ltd., Singapore.

BORN, K., A. FINK, H. PAETH, 2008: Dry and wet periods in the northwestern Maghreb for present day and future climate conditions. – Meteorol. Z. **17**, 533–551.

BRUNETTI, M., M. COLACINO, M. MAUGERI, T. NANNI, 2001: Trends in the daily intensity of precipitation in Italy from 1951 to 1996. – Int. J. Climatol. **21**, 299–316.

BUSUIOC, A., R. TOMOZEIU, C. CACCIAMANI, 2008: Statistical downscaling model based on canonical correlation analysis for winter extreme precipitation events in the Emilia-Romagna region. – Int. J. Climatol. **28**, 449–464.

CAVAZOS T., B.C. HEWITSON, 2005: Performance of NCEP-NCAR reanalysis variables in statistical downscaling of daily precipitation. – Climate Res. **28**, 95–107.

DAI, A., 2006: Precipitation characteristics in eighteen coupled climate models. – J. Climate **19**, 4605–4630.

DÉQUÉ, M., R.G. JONES, M. WILD, F. GIORGI, J.C. CHRISTENSEN, D.C. HASSELL, P.L. VIDALE, B. ROCKEL, D. JACOB, E. KJELLSTROM, M. DE CASTRO, F. KUCHARSKI, B. VAN DEN HURK, 2005: Global high resolution versus Limited Area Model climate change projections over Europe: quantifying confidence level from PRUDENCE results. – Climate Dynam. **25**, 653–670.

DIRMEYER, P.A., X. GAO, M. ZHAO, Z. GUO, T. OKI, N. HANASAKI, 2006: The second global soil wetness project (GSWP-2): multi-model analysis and implications for our perception of the land surface. – Bull. Amer. Meteor. Soc. **87**, 1381–1397.

DÜNKELOH, A., J. JACOBEIT, 2003: Circulation Dynamics of Mediterranean Precipitation Variability 1948–1998. – Int. J. Climatol. **23**, 1843–1866.

DURMAN, C.F., J.M. GREGORY, D.C. HASSELL, R.G. JONES, J.M. MURPHY, 2001: A comparison of extreme European daily precipitation simulated by a global model and regional climate model for present and future climates. – Quart. J. Roy. Meteor. Soc. **127**, 1005–1015.

EMORI, S., A. HASEGAWA, T. SUZUKI, K. DAIRAKU, 2005: Validation, parameterization dependence and future projection of daily precipitation simulated with an atmospheric GCM. – Geophys. Res. Lett. **32**, L06708, DOI:10.1029/2004GL022306.

FOWLER, H.J., M. EKSTRÖM, S. BLENKINSOP, A.P. SMITH, 2007: Estimating change in extreme European precipitation using a multimodel ensemble. – J. Geophys. Res. **112**, D18104, DOI:10.1029/2007JD008619.

FREI, C., R. SCHÖLL, S. FUKUTOME, J. SCHMIDLI, P.L. VIDALE, 2006: Future change of precipitation extremes in Europe: Intercomparison of scenarios from regional climate models. – J. Geophys. Res. **111**, D06105, DOI:10.1029/2005JD005965.

GAO, X., J.S. PAL, F. GIORGI, 2006: Projected changes in mean and extreme precipitation over the Mediterranean region from high resolution double nested RCM simulations. – Geophys. Res. Lett. **33**, L03706.

GIORGI, F., 2006: Climate change hot-spots. – Geophys. Res. Lett. **33**, L08707, DOI:10.1029/2006GL025734.

GIORGI, F., P. LIONELLO, 2008: Climate change projections for the Mediterranean area. – Global Planet. Change **63**, 90–104.

HAYLOCK, M.R., N. HOFSTRA, A.M.G. KLEIN TANK, E.J. KLOK, P.D. JONES, M. NEW, 2008: A European daily high-resolution gridded dataset of surface temperature and precipitation. – J. Geophys. Res. Atmos. **113**, D20119, DOI:10.1029/2008JD10201.

HERTIG, E., J. JACOBEIT, 2008: Assessments of Mediterranean precipitation changes for the 21st century using statistical downscaling techniques. – Int. J. Climatol. **28**, 1025–1045.

HERTIG, E., S. SEUBERT, J. JACOBEIT, 2010: Temperature extremes in the Mediterranean area: Trends in the past and assessments for the future. – Nat. Hazards Earth Syst. Sci. **10**, 2039–2050.

HEWITSON, B.C., 1998: Regional climate downscaling from GCMs. – Report K751, Water Research Commission, Pretoria, South Africa.

HOUGHTON J.T., Y. DING, D.J. GRIGGS, M. NOGUER, P.J. VAN DER LINDEN, D. XIAOSU (Eds.), 2001: Climate Change 2001: The Scientific Basis. Contribution of the Working Group I to the Third Assessment Report of the Intergovernmental Panel on Climate Change (IPCC). – Cambridge University Press, Cambridge, 944 pp.

JACOB, D., L. BÄRRING, O.B. CHRISTENSEN, J.H. CHRISTENSEN, M. DE CASTRO, M. DÉQUÉ, F. GIORGI, S. HAGEMANN, M. HIRSCHI, R. JONES, E. KJELLSTRÖM, G. LENDERINK, B. ROCKEL, C. SCHÄR, S.I. SENEVIRATNE, S. SOMOT, A. VAN ULDEN, B. VAN DEN HURK, 2007: An inter-comparison of regional climate models for Europe: model performance in present day climate. – Climatic Change **81**, 31–52.

KALNAY, E., M. KANAMITSU, R. KISTLER, W. COLLINS, D. DEAVEN, L. GANDIN, M. IREDELL, S. SAHA, G. WHITE, J. WOOLLEN, Y. ZHU, M. CHELLIAH, W. EBISUZAKI, W. HIGGINS, J. JANOWIAK, K.C. MO, C. ROPELEWSKI, J. WANG, A. LEETMAA, R. REYNOLDS, R. JENNE, D. JOSEPH, 1996: The NCEP/NCAR 40-Year Reanalysis Project. – Bull. Amer. Meteor. Soc. **77**, 437–471.

KENDON, E.J., D.P. ROWELL, R.G. JONES, 2010: Mechanisms and reliability of future projected changes in daily precipitation. – Climate Dynam. **35**, 489–509.

KIDSON, J.W., C.S. THOMPSON, 1998: Comparison of statistical and model-based downscaling techniques for estimating local climate variations. – J. Climate **11**, 735–753.

KISTLER, R., E. KALNAY, W. COLLINS, S. SAHA, G. WHITE, J. WOOLLEN, M. CHELLIAH, W. EBISUZAKI, M. KANAMITSU, V. KOUSKY, H. VAN DEN DOOL, R. JENNE, M. FIORINO, 2001: The NCEP/NCAR 50-Year Reanalysis: Monthly Means CD-ROM and Documentation. – Bull. Amer. Meteor. Soc. **82**, 247–268.

KOSTOPOULOU, E., P.D. JONES, 2005: Assessment of climate extremes in the Eastern Mediterranean. – Meteorol. Atmos. Phys. **89**, 69–85.

KUTIEL, H., T.R. HIRSCH-ESHKOL, M. TÜRKES, 2001: Sea level pressure patterns associated with dry or wet monthly rainfall conditions in Turkey. – Theor. Appl. Climatol. **69**, 39–67.

LIONELLO P., U. BOLDRIN, F. GIORGI, 2008: Future changes in cyclone climatology over Europe as inferred from a regional climate simulation. – Climate Dynam. **30**, 657–671.

LOPEZ-BUSTINS, J.-A., J. MARTIN-VIDE, A. SANCHEZ-LORENZO, 2008: Iberia winter rainfall trends based upon changes in teleconnection and circulation patterns. – Global Planet. Change **63**, 171–176.

MAHERAS, P., E. XOPLAKI, H. KUTIEL, 1999: Wet and dry monthly anomalies across the Mediterranean basin and their relationship with circulation, 1860–1990. – Theor. Appl. Climatol. **64**, 189–199.

MANN, H.B., D.R. WHITHNEY, 1947: On a test whether one of two random variables is stochastically larger than the other. – Ann. Math. Statist. **18**, 50–60.

MEEHL, G.A., T.F. STOCKER, W.D. COLLINS, P. FRIEDLINGSTEIN, A.T. GAYE, J.M. GREGORY, A. KITOH, R. KNUTTI, J.M. MURPHY, A. NODA, S.C.B. RAPER, I.G. WATTERSON, A.J. WEAVER AND Z.-C. ZHAO, 2007: Global Climate Projections. – In: SOLOMON, S., D. QIN, M. MANNING, Z. CHEN, M. MARQUIS, K.B. AVERYT, M. TIGNOR, H.L. MILLER (Eds.): Climate Change 2007: The Physical Science Basis. Contribution of Working Group I to the Fourth Assessment Report of the Intergovernmental Panel on Climate Change. – Cambridge University Press, Cambridge, United Kingdom and New York, NY, USA.

MOBERG, A., P.D. JONES, D. LISTER, A. WALTHER, M. BRUNET, J. JACOBEIT, L.V. ALEXANDER, P. DELLA-MARTA, J. LUTERBACHER, P. YIOU, D. CHEN, A. KLEIN TANK, O. SALADIÉ, J. SIGRÓ, E. AGUILAR, H. ALEXANDERSSON, C. ALMARZA, I. AUER, M. BARRIENDOS, M. BEGERT, H. BERGSTRÖM, R. BÖHM, C. J. BUTLER, J. CAESAR, A. DREBS, D. FOUNDA, F.-W. GERSTENGARBE, G. MICELA, M. MAUGERI, H. ÖSTERLE, K. PANDZIC, M. PETRAKIS, L. SRNEC, R. TOLASZ, H. TUOMENVIRTA, P.C. WERNER, H. LINDERHOLM, A. PHILIPP, H. WANNER, E. XOPLAKI, 2006: Indices for daily temperature and precipitation extremes in Europe analysed for the period 1901–2000. – J. Geophys. Res.-Atmos. **111**, D22106, DOI:10.1029/2006JD007103.

NAKICENOVIC, N., R. SWART (Eds.), 2000: Emissions Scenarios 2000. Special Report of the Intergovernmental Panel on Climate Change. – Cambridge University Press, Cambridge, 570 pp.

PAETH, H., M. DIEDERICH, 2010: Postprocessing of simulated precipitation for impact research in West Africa. Part II: A weather generator for daily data. – Climate Dynam., published online, DOI: 10.1007/s00382-010-0840-0.

PAETH, H., A. HENSE, 2005: Mean versus extreme climate in the Mediterranean region and its sensitivity to future global warming conditions. – Meteorol. Z. **14**, 329–347.

PAETH, H., K. BORN, R. GIRMES, R. PODZUN, D. JACOB, 2009: Regional climate change in tropical and northern Africa due to greenhouse forcing and land use changes. – J. Climate **22**, 114–132.

PAXIAN, A., E. HERTIG, G. VOGT, S. SEUBERT, J. JACOBEIT, H. PAETH, in review: Validation and interpretation of regional climate model trends in the Mediterranean area in the context of mid-latitude circulation variability. – Climate Dynam.

PHILIPP A., P.M. DELLA-MARTA, J. JACOBEIT, D. R. FEREDAY, P. D. JONES, A. MOBERG, H. WANNER, 2007: Long term variability of daily North Atlantic-European pressure patterns since 1850 classified by simulated annealing clustering. – J. Climate **20**, 4065–4095.

PREISENDORFER, R.W., 1988: Principal Component Analysis in Meteorology and Oceanography. – Develop. Atmos. Sci. **17**, Amsterdam.

RAIBLE, CH.C., B. ZIV, H. SAARONI, M. WILD, 2010: Winter synoptic-scale variability over the Mediterranean Basin under future climate conditions as simulated by the ECHAM5. – Climate Dynam. **35**, 473–488.

RAO, C.R., 1973: Linear statistical inference and its applications. – Wiley series in probability and mathematical statistics, Wiley New York, 625 pp.

RAPP, J., C.-D. SCHÖNWIESE, 1995: Atlas der Niederschlags- und Temperaturtrends in Deutschland 1891–1990. – Frankfurter Geowissenschaftliche Arbeiten, Serie B, Band 5, Frankfurt.

RICHMAN, M.B., 1986: Rotation of principal components. – J. Climatol. **6**, 293–335.

ROECKNER, E., K. ARPE, L. BENGTSSON, M. CHRISTOPH, M. CLAUSSEN, L. DUMENIL, M. ESCH, M. GIORGETTA, U. SCHLESE, U. SCHULZWEIDA, 1996: The atmospheric general circulation model ECHAM-4: Model description and simulation of present-day climate. – Max Planck Institute for Meteorology Report **218**, Hamburg.

ROECKNER, E., G. BAEUML, L. BONAVENTURA, R. BROKOPF, M. ESCH, M. GIORGETTA, S. HAGEMANN, I. KIRCHNER, L. KORNBLUEH, E. MANZANI, A. RHODIN, U. SCHLESE, U. SCHULZWEIDA, A. TOMPKINS, 2003: The atmospheric general circulation model ECHAM5. Part I: Model description. – Max Planck Institute for Meteorology Report **349**, Hamburg.

ROECKNER, E., G.P. BRASSEUR, M. GIORGETTA, D. JACOB, J. JUNGCLAUS, C. REICK, J. SILLMANN, 2006: Climate projections for the 21st century. – Max Planck Institute for Meteorology, Hamburg.

SANCHEZ-GOMEZ, E., S. SOMOT, M. DEQUE, 2009: Ability of an ensemble of regional climate models to reproduce weather regimes over Europe-Atlantic during the period 1961–2000. – Climate Dynam. **33**, 723–736.

SCHMIDLI, J., C. FREI, P.L. VIDALE, 2006: Downscaling from GCM precipitation: a benchmark for dynamical and statistical downscaling methods. –Int. J. Climatol. **26**, 679–689.

SILLMANN, J., E. ROECKNER, 2008: Indices for extreme events in projections of anthropogenic climate change. – Climatic Change **86**, 83–104.

TEBALDI, C., K. HAYHOE, J.M. ARBLASTER, G.A. MEEHL, 2006: Going to the extremes. An intercomparison of model-simulated historical and future changes in extreme events. – Climatic Change **79**, 185–211.

TORETI, A., E. XOPLAKI, D. MARAUN, F.G. KUGLITSCH, H. WANNER, J. LUTERBACHER, 2010: Characterisation of extreme winter precipitation in Mediterranean coastal sites and associated anomalous atmospheric circulation patterns. – Nat. Hazards Earth Syst. Sci. **10**, 1037–1050.

VON STORCH, H., F.W. ZWIERS, 1999: Statistical Analysis in Climate Research. – Cambridge University Press, Cambridge, 484 pp.

VON STORCH, H., E. ZORITA, U. CUBASCH, 1993: Downscaling of Global Climate Change Estimates to Regional Scales: An Application to Iberian Rainfall in Wintertime. – J. Climate **6**, 1161–1171.

VRAC, M., P. NAVEAU, 2007: Stochastic downscaling of precipitation: From dry events to heavy rainfall. – Water Resour. Res. **43**, W07402,DOI:10.1029/2006WR005308.

WILBY, R.L., 1998: Statistical downscaling of daily precipitation using daily airflow and seasonal teleconnection indices. – Climate Res. **10**, 163–178.

XOPLAKI, E., J.F. GONZÁLEZ-ROUCO, J. LUTERBACHER, H. WANNER, 2004: Wet season Mediterranean precipitation variability: Influence of large-scale dynamics. – Climate Dynam. **23**, 63–78.